

# Analysis of the Golgi Apparatus in *Arabidopsis* Seed Coat Cells during Polarized Secretion of Pectin-Rich Mucilage <sup>WJCA</sup>

Robin E. Young,<sup>a</sup> Heather E. McFarlane,<sup>b</sup> Michael G. Hahn,<sup>c</sup> Tamara L. Western,<sup>b</sup> George W. Haughn,<sup>a</sup> and A. Lacey Samuels<sup>a,1</sup>

<sup>a</sup>Department of Botany, University of British Columbia, Vancouver, Canada V6T 1Z4

<sup>b</sup>Department of Biology, McGill University, Montreal, Canada H3A 1B1

<sup>c</sup>Complex Carbohydrate Research Center and Department of Plant Biology, University of Georgia, Athens, Georgia 30602

**Differentiation of the *Arabidopsis thaliana* seed coat cells includes a secretory phase where large amounts of pectinaceous mucilage are deposited to a specific domain of the cell wall. During this phase, Golgi stacks had cisternae with swollen margins and *trans*-Golgi networks consisting of interconnected vesicular clusters. The proportion of Golgi stacks producing mucilage was determined by immunogold labeling and transmission electron microscopy using an antimucilage antibody, CCRC-M36. The large percentage of stacks found to contain mucilage supports a model where all Golgi stacks produce mucilage synchronously, rather than having a subset of specialist Golgi producing pectin product. Initiation of mucilage biosynthesis was also correlated with an increase in the number of Golgi stacks per cell. Interestingly, though the morphology of individual Golgi stacks was dependent on the volume of mucilage produced, the number was not, suggesting that proliferation of Golgi stacks is developmentally programmed. Mapping the position of mucilage-producing Golgi stacks within developing seed coat cells and live-cell imaging of cells labeled with a *trans*-Golgi marker showed that stacks were randomly distributed throughout the cytoplasm rather than clustered at the site of secretion. These data indicate that the destination of cargo has little effect on the location of the Golgi stack within the cell.**

## INTRODUCTION

The secretory system of plants is integral to the synthesis and deposition of many cell wall components, including pectin (Doblin et al., 2003). The plant Golgi apparatus is comprised of large numbers of individual Golgi stacks, which are widely distributed throughout the cytoplasm and are capable of streaming, a process mediated by the actin cytoskeleton (Griffing, 1991; Boevink et al., 1998; Nebenführ et al., 1999). During the late stages of mitosis, the Golgi apparatus proliferates and plays an integral role in the synthesis of the cell plate between daughter cells (Hirose and Komamine, 1989; Jürgens, 2005; Segui-Simarro and Staehelin, 2006). The capacity for Golgi streaming seen in plants and many other eukaryotes could result in the use of strategies for delivery of cargo to and from the Golgi that are not available to species in which the Golgi is maintained in a single, centralized position (Nebenführ and Staehelin, 2001). Not only do plant Golgi stacks have the capacity to travel to the site of deposition if needed, but also targeting of vesicles to and from the Golgi is complicated by the fact that Golgi stacks are in motion.

Much of the cargo that passes through the plant secretory pathway to the plasma membrane is comprised of cell wall polysaccharides synthesized in the Golgi. The plant cell wall is a dynamic extracellular matrix, and its organization is integral to its proper function (Somerville et al., 2004; Cosgrove, 2005). The current model for primary cell wall structure proposes a series of macromolecular networks that are intertwined and interconnected to provide the strength and support (Carpita and Gibeaut, 1993; Carpita and McCann, 2000) necessary for the plant to withstand both tension and compression, while at the same time having the ability to grow in a precisely controlled and directed manner (Jarvis and McCann, 2000). One such network is thought to consist of cellulose and hemicellulose. In the *Arabidopsis thaliana* primary cell wall, the predominant hemicellulose is xyloglucan (XG). Unlike the plasma membrane-localized synthesis of cellulose, XG has been shown to be synthesized inside the Golgi and then secreted to the outside of the plasma membrane via vesicular transport (Moore et al., 1991). The hemicellulose-cellulose framework described above is thought to be embedded in a second macromolecular network, namely, a gel matrix composed primarily of pectic polysaccharides, such as homogalacturonans, rhamnogalacturonan I (RGI), and rhamnogalacturonan II. Pectin biosynthesis is also a Golgi-mediated process, as first shown by autoradiography (Northcote and Pickett-Heaps, 1966).

The use of antibodies has further expanded our understanding of the flexibility of the Golgi apparatus in the synthesis of cell wall polysaccharide/glycoprotein components, though there is still much that is unknown. Zhang and Staehelin (1992) found that the

<sup>1</sup> Address correspondence to lsamuels@interchange.ubc.ca.

The author responsible for distribution of materials integral to the findings presented in this article in accordance with the policy described in the Instructions for Authors (www.plantcell.org) is: A. Lacey Samuels (lsamuels@interchange.ubc.ca).

<sup>WJCA</sup>Online version contains Web-only data.

<sup>Open Access</sup>Open Access articles can be viewed online without a subscription. www.plantcell.org/cgi/doi/10.1105/tpc.108.058842

production of cell wall polysaccharides in suspension-cultured cells, which are constitutively secreting cell wall components to all regions of the plasma membrane, is a stepwise process occurring from *cis* to *trans* and that different products can be synthesized in the same Golgi stack. A separate study showed that transport vesicles in clover root tips, another diffusely secreting cell type, can carry both XG and RGI epitopes at the same time (Lynch and Staehelin, 1992). In the *Arabidopsis* root cap, the ultrastructure of the Golgi apparatus was observed to undergo changes that were consistent with the increased levels of secretion that occur as the meristematic cells differentiate into mucilage producing cells (Staehelin et al., 1990). However, in all cases described above, increases in the numbers of Golgi stacks in a given cell, as a possible mechanism for accommodating increased levels of secretion, were not determined.

*Arabidopsis* seeds synthesize and secrete large amounts of pectinaceous mucilage to the extracellular space during a specific time period of seed maturation (between 6 and 8 d postanthesis [DPA]). The mucilage is secreted into a donut-shaped pocket at the junction of the radial and outer tangential walls of the epidermal cells of the seed coat (Beeckman et al., 2000; Western et al., 2000; Windsor et al., 2000). Following mucilage secretion, the epidermal cells synthesize a thick cellulosic secondary cell wall (9 to 11 DPA), which is laid down across the apical surface of the cytoplasm. This results in the formation of a volcano-shaped protrusion through the center of the mucilage pocket at seed maturity. A number of mutants with defects in the capacity of these cells to produce and/or secrete mucilage have been studied, including *mucilage modified4* (*mum4*) (Western et al., 2001, 2004), in which the production of mucilage in the seed coat has been disrupted. The *MUM4* gene encodes a putative rhamnose synthase that is upregulated during the mucilage-producing stage of seed coat development (Usadel et al., 2004; Western et al., 2004).

In this article, we have investigated how the secretory system can accommodate striking changes in both the amount and type of cell wall polysaccharide being produced by the Golgi apparatus. The onset of enhanced polysaccharide production was accompanied by a dramatic increase in the number and structure of Golgi stacks in the seed coat cells. The ultrastructural changes in the Golgi were dependent on the volume of mucilage being produced, as mutants lacking mucilage did not have the characteristic morphology of the wild type. However, the number of Golgi stacks observed in the cell was not dependent on mucilage production, as the Golgi number in *mum4* mutants still increased in a developmentally appropriate manner. The mucilage-containing Golgi stacks were not clustered near the site of secretion but were instead randomly distributed throughout the cell. These data demonstrate that, although the plant Golgi is made up of scattered stacks, the Golgi apparatus as a whole responds to developmental cues and surges in production as a coordinated unit.

## RESULTS

### Seed Coat Cells Undergo Distinct Ultrastructural Rearrangements during Differentiation

An overview of seed coat cell differentiation was undertaken to examine the organellar rearrangements that occur in the whole

cell and to put polysaccharide production and secretion into this context. *Arabidopsis* seeds were excised from siliques and high pressure frozen before (at 4 DPA), during (at 7 DPA), and after (at 9 DPA) the mucilage-producing stages of seed coat development and the ultrastructure, specifically in the Golgi apparatus, were examined.

Prior to the mucilage-secreting phase (4 DPA), epidermal cells had a large central vacuole, a nucleus typically located at the basolateral side of the cell, and amyloplasts (containing starch granules) that were either basal or apical (Figure 1A). Golgi stacks were seen in the narrow cytosolic region surrounding the vacuole. Cisternae were long and relatively thin, and the *trans*-Golgi network (TGN) was small, compared with other stages of development (Figure 1B). In many cases, the Golgi appeared cup-shaped, with the TGN on the concave surface.

During mucilage secretion (7 DPA), seed coat epidermal cells had well-developed, ring-shaped mucilage pockets between the plasma membrane and primary cell wall, with the vacuole limited to the lower portion of the cell (Figure 1C). The nucleus and starch granules were positioned in the upper portion of the cytoplasmic column. Interestingly, microtubules were seen lining the membrane on the cytosolic side of the mucilage pocket but not in other regions of the cell (McFarlane et al., 2008). The Golgi stack morphology at 7 DPA differed from the 4 DPA morphology in that the stacks had a shorter diameter than those observed at 4 DPA, and the *cis-trans* polarity across the stack was more pronounced. The lumen of the *cis* cisternae was wider, while the medial and *trans* cisternae had compressed lumens, like those at 4 DPA, except with swollen margins (cf. Figures 1B and 1D). In addition, there appeared to be more TGN and more large vesicles associated with the TGN (Figure 1D).

Considering that a large, convoluted TGN might be difficult to capture in thin sections, as connections between portions of the TGN might be outside of the plane of section, electron tomography was used to examine the morphology of the 7-DPA Golgi stack in greater detail. Models that had been built from three different tomograms showed that much of what appeared to be free vesicles near the TGN in thin sections were interconnected vesicular clusters (Figure 2). During the intense secretion of mucilage that is characteristic of 7-DPA seed coat cells, the swollen vesicular regions of the TGN lacked obvious coats and were large (~200 nm). This is morphologically distinct from the partially coated reticulum, an interconnected cluster of coated vesicles, with dilations that are approximately half the size of those described here (Pesacreta and Lucas, 1985). The clusters in this study appeared to be budding from flattened cisternal domains, suggesting that these sites represent the exit site of the Golgi stack (Figures 2C and 2D). The TGN-interconnected vesicular clusters were immediately adjacent to the *trans*-most cisterna, in agreement with the results of Sequi-Simarro and Staehelin (2006), where all TGN and Golgi stacks in meristematic cells were tracked, demonstrating the proximal arrangement of TGN to Golgi stacks.

After the secretion of mucilage ended (9 DPA), seed coat cells had a distinguishable layer of secondary cell wall lining the apical side of the cell, between the mucilage pocket and the plasma membrane and along the top of the cytoplasmic column (Figure 1E). The vacuole was still located at the basal side of the cell but

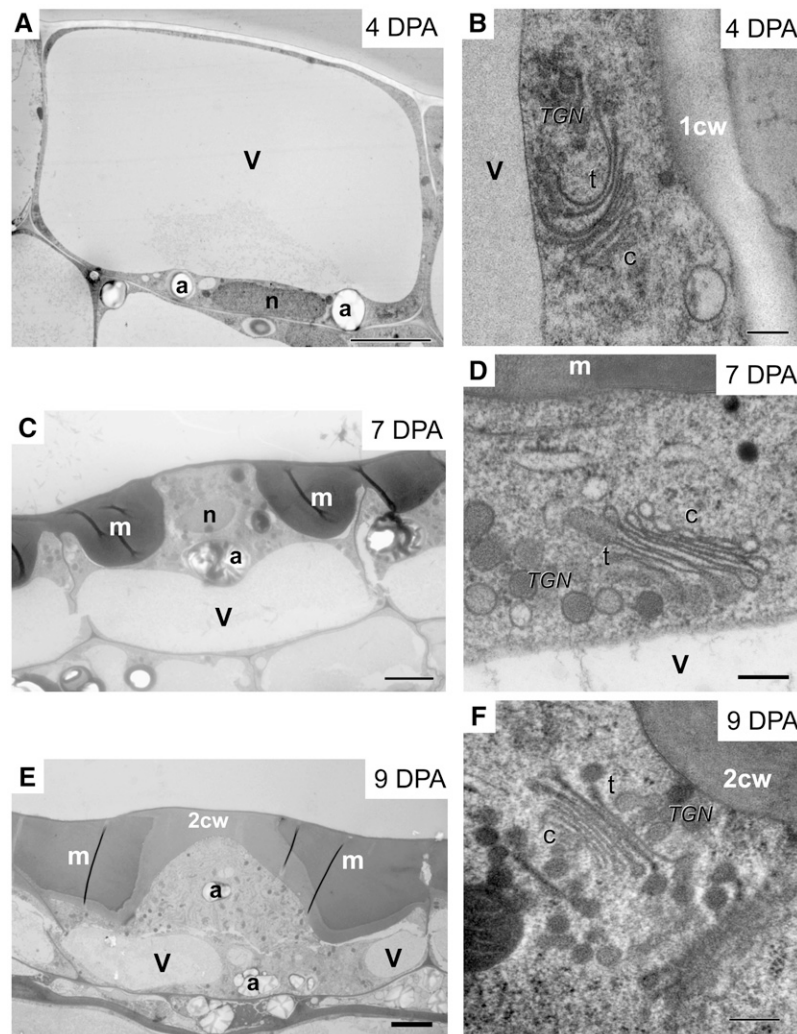


**Figure 1.** The Stages of *Arabidopsis* Seed Coat Development in Cryofixed Samples.

(A) Cells (4 DPA) are relatively undifferentiated, with a large central vacuole.

(B) Detail of a 4-DPA Golgi stack.

(C) Cells (7 DPA) show the characteristic mucilage pocket, forming a ring around a central cytoplasmic column.

(D) Detail of a 7-DPA Golgi stack.

(E) Cells (9 DPA) have secondary cell wall on the apical side of the cell.

(F) Detail of a 9-DPA Golgi stack.

a, amyloplast; c, *cis* face of Golgi stack; 1cw, primary cell wall; 2cw, secondary cell wall; m, mucilage; n, nucleus; t, *trans* face of Golgi stack; V, vacuole. Bars = 5  $\mu$ m in (A), (C), and (E) and 250 nm in (B), (D), and (F).

appeared smaller in volume. Microtubules around the mucilage pocket were not prominent at this stage. Golgi stacks were similar to those seen in 7-DPA cells, exhibiting short, compressed cisternae with swollen margins and extensive TGN (Figure 1F).

#### **Antibodies to Mucilage Components Demonstrate That Plant Golgi Stacks Produce Mucilage Synchronously during Seed Coat Epidermal Differentiation**

Previous work has shown that different antipectin antibodies can be used to label hydrated, extruded mucilage from mature seeds

(Willats et al., 2001a; Western et al., 2004; Macquet et al., 2007). To follow mucilage secretion within the cell, we required an antibody that reacted strongly with mucilage in cryofixed, resin-embedded, sectioned material. We initially tested a range of antibodies for their ability to bind extruded mucilage (see Methods for comprehensive list). Though there was a number of antibodies from this screen that were capable of binding hydrated mucilage in mature seeds (see Supplemental Figure 1 online), only two of those were capable of binding to mucilage in cryofixed, sectioned material (CCRC-M36 and antixyloglucan [ $\alpha$ -XG]; Figures 3, 4, and 6A). Thus, CCRC-M36 and  $\alpha$ -XG were chosen to investigate changes

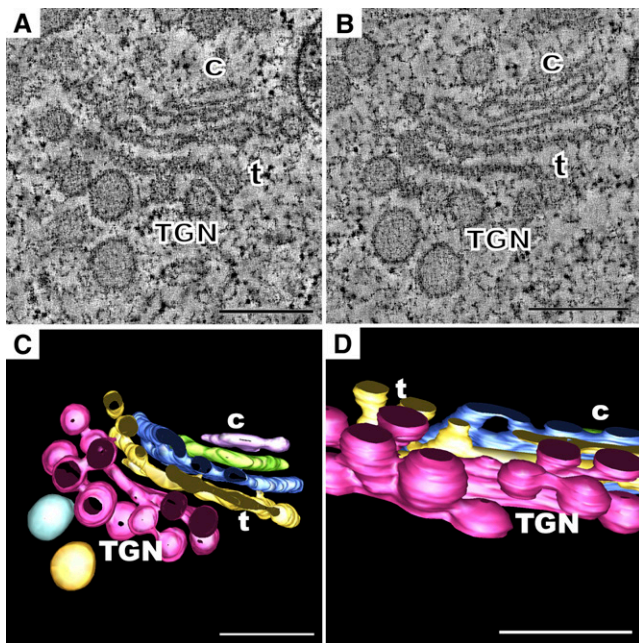


**Figure 2.** Tomographic Reconstruction of a Single Golgi Stack during the Mucilage-Secreting Phase of an *Arabidopsis* Seed Coat Cell (7 DPA).

(A) and (B) Slices (2 nm) from a tomogram, showing how the TGN appears as a series of vesicles.

(C) and (D) En face (C) and side (D) view of a three-dimensional model of a Golgi stack, based on tomographic reconstruction shown in (A) and (B). The TGN (bright pink) is an extensive interconnected network of large vesicle-like structures.

c, cis face of Golgi stack; t, trans face of Golgi stack. Bars = 250 nm.

in polysaccharide product by immunolabeling sections of seeds before, during, and after mucilage production.

To study pectinaceous mucilage, an ideal probe would react strongly with the pectin of the mucilage but only weakly or not at all with the pectins of the cell wall. CCRC-M36 is a monoclonal antibody raised against *Arabidopsis* seed coat mucilage, and it binds strongly to RGIs from *Arabidopsis*, tomato (*Solanum lycopersicum*), lettuce (*Lactuca sativa*), and soybean (*Glycine max*) as well as to *Arabidopsis* and mustard (*Sinapis alba*) seed coat mucilages (T. Bootten, Z. Popper, A.G. Swennes, and M.G. Hahn, unpublished data). Its epitope appears to reside on the unbranched backbone of RGI, and it does not bind strongly with arabinogalactans, xylans, XGs, or methyl-esterified homogalacturonans (C. Deng, R. Jia, A. Albert, W.S. York, M.A. O'Neill, and M.G. Hahn, unpublished data). At 4 DPA (Figure 3A), prior to the onset of mucilage production, CCRC-M36 showed no reactivity to any cell walls in cryofixed, sectioned seeds, including specifically the seed coat cells (Figure 3D). At 7 DPA (Figures 3B and 4A), at the height of mucilage production, the mucilage pockets of seed coat cells between the primary cell wall and plasma membrane were brightly labeled, but the cell walls of these and other cell types were not (Figures 3E and 4C). Punctate structures were observed in the cytosol of 7-DPA seed coat cells but not at 9 DPA (Figures 4C and 4D), when polysaccharide production had shifted from the production of mucilage to the produc-

tion of secondary cell wall (Figures 3C and 4B). Labeling of the mature mucilage pockets was strong in 9-DPA seed coat cells (Figures 3F and 4D).

To contrast with the binding of CCRC-M36 to mucilage, an antibody that reacted with the cell wall was required. Though a number of typical cell wall antibodies were tested against primary and secondary cell wall components, the only antibody that exhibited any reactivity to the seed coat cell wall was a polyclonal  $\alpha$ -XG (Figures 4E and 4F). This antibody was raised against sycamore maple (*Acer pseudoplatanus*) XG and does not cross-react with pectic components, like RGI (Moore and Staehelin, 1988). In addition to the labeling of developing secondary cell walls in the *Arabidopsis* seed coat, this antibody also labeled primary cell walls of the seed throughout development, and the mucilage pockets, but at a less intense level than CCRC-M36 (Figures 3G to 3I and 6A). Due to the nature of the cellulose-hemicellulose network, these results suggested that cellulose might also be present in mucilage. The presence of cellulose was confirmed by labeling hydrated, extruded mucilage with cellulose binding domain, conjugated to the fluorescent molecule Oregon Green (CBD-OG; see Supplemental Figure 1D online), a result which is consistent with the study of Macquet et al. (2007).

The changes in the CCRC-M36 labeling patterns observed in 7-DPA seed coat cells indicated that a closer examination of the secretory apparatus might yield new information about the regulation of the secretory pathway during seed coat development. Since CCRC-M36 labels only mucilage and not other primary cell wall components in this cell type, this antibody was used to identify the specific population of Golgi stacks that are involved in the production of mucilage during seed coat development. To resolve the puncta observed in fluorescence microscopy and to quantify individual Golgi stacks producing mucilage, sections of 7- and 9-DPA seeds were immunolabeled with either CCRC-M36 or  $\alpha$ -XG together with gold-conjugated secondary antibodies for examination by transmission electron microscopy (TEM) (Figure 5). CCRC-M36 labeled 70% of all Golgi stacks visible in 7-DPA seed coat sections, most commonly labeling the medial and/or trans cisternae as well as the TGN. By contrast, 0% of Golgi stacks were labeled by CCRC-M36 in 9-DPA cells. These data indicate that the pectin epitope is indeed present in the Golgi during a short period of intense mucilage secretion but not at later stages during synthesis of the secondary cell wall. Thus, the short-term, specialized production of mucilage is reflected in the pattern of Golgi labeling. On the other hand, when  $\alpha$ -XG was used as the primary antibody, gold particles were seen associated with 16% of Golgi stacks in 7-DPA cells, and 22% of Golgi stacks in 9-DPA cells, suggesting that XG is secreted during the synthesis of both the mucilage and columella.

Despite the high percentage of Golgi stacks that label with CCRC-M36 at 7 DPA, it is conceivable that the epitopes recognized by the two different antibodies are being carried by different groups of Golgi stacks. To address this question, double labeling experiments, using both CCRC-M36 and  $\alpha$ -XG, were performed on 7-DPA seed coat cells (Figure 6). Results of double labeling were consistent with single labeling assays; 77% of Golgi stacks labeled with CCRC-M36 in the double labeling experiment, whereas 11% of Golgi stacks labeled with  $\alpha$ -XG. Of the six Golgi stacks observed to have  $\alpha$ -XG label, only one of

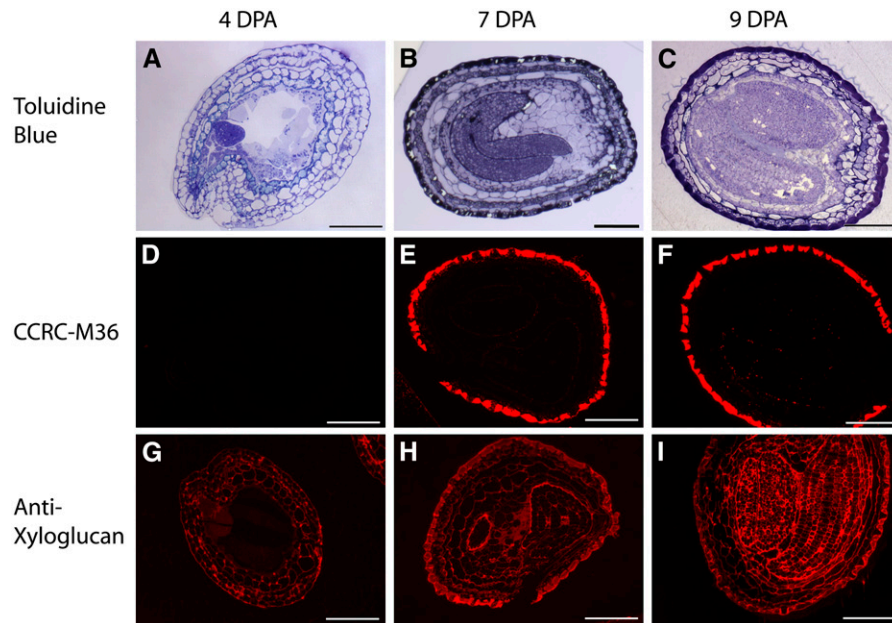


**Figure 3.** Distribution of Seed Mucilage (CCRC-M36) or XG ( $\alpha$ -XG) Epitopes in Developing *Arabidopsis* Seeds.

(A) to (C) Toluidine blue-stained sections show seed anatomy at 4, 7, and 9 DPA.

(D) to (F) Sections of 4-, 7-, and 9-DPA seeds fluorescently immunolabeled with CCRC-M36. CCRC-M36 labels only 7 (E) and 9 (F) DPA seed coat cells.

(G) to (I) Sections of 4-, 7-, and 9-DPA seeds immunolabeled with  $\alpha$ -XG.  $\alpha$ -XG labels primary cell walls of seed coats at all time points, in addition to the label observed in mucilage at 7 (H) and 9 (I) DPA.

Bars = 100  $\mu$ m.

them did not also have CCRC-M36 label, suggesting that the different antibodies do not identify distinct groups of Golgi stacks within the cell.

### The Number of Golgi Stacks in the Cell Increases during Mucilage Production

To determine whether the onset of mucilage production resulted in changes in the number of individual stacks in the Golgi apparatus, the number of Golgi stacks in 4-, 7-, and 9-DPA cells was quantified. This was done using a twofold approach. First, high-resolution TEM of seed coat cells at each developmental stage was undertaken to count Golgi stacks in seed coat cells directly. When thin sections of seed coat cells were examined in TEM, an increase in the number of Golgi stacks was observed (Figure 7A). However, during the same period (between 4 and 7 DPA), seed coat cells underwent dramatic cytosolic rearrangements (cf. Figures 1A and 1C), which manifested as an increase in the surface area of cytoplasm visible in thin sections between 4 and 7 DPA (Figure 7B). Thus, the surface area of cytoplasm available for quantification at 4 DPA was significantly less than at 7 DPA, which could have resulted in an underrepresentation of the true number of Golgi stacks present in 4-DPA cells. For this reason, we determined the density of Golgi stacks (number of Golgi stacks/ $\mu$ m<sup>2</sup>) visible in our sections by dividing the absolute number of stacks by the cytoplasmic surface area (Figure 7C). Three-way analysis of Golgi density at 4, 7, and 9 DPA showed statistically significant differences [Kruskal-Wallis test;  $H(2) =$

66.94,  $P < 0.05$ ]. Post hoc analysis using the Mann-Whitney test showed a significant increase in the density of Golgi stacks at 7 DPA compared with 4 DPA (Mann-Whitney  $U = 326.0$ ,  $P < 0.025$ ). The number of Golgi stacks/ $\mu$ m<sup>2</sup> approximately doubled between 4 and 7 DPA (0.08 stacks/ $\mu$ m<sup>2</sup> versus 0.14 stacks/ $\mu$ m<sup>2</sup>, respectively). By contrast, when the density of Golgi stacks in 7- and 9-DPA seed coat cells were compared, no significant differences were found. This demonstrates that an increase in the number of Golgi stacks found in seed coat cells is correlated with the increase in polysaccharide production at the onset of mucilage secretion.

The second method that was used to quantify Golgi stacks was live imaging of Golgi stacks in whole seed coat cells via fluorescent molecular markers for the Golgi. Developing seeds were dissected from siliques of transgenic *Arabidopsis* plants bearing the *trans*-Golgi marker sialyl transferase conjugated to green fluorescent protein (ST-GFP), driven by the constitutive 35S promoter (Boevink et al., 1998). Despite reports that the 35S promoter results in gene expression in all tissues (Odell et al., 1985), the expression of ST-GFP in the *Arabidopsis* seed coat was patchy, with only a few cells in each seed coat displaying fluorescence (Figure 8A). In cells that exhibited fluorescence, punctate structures of the correct size and shape as Golgi stacks were observed (Figure 8). These puncta were mobile but did not display the rapid long-distance streaming that has been observed in fluorescent Golgi stacks in *Nicotiana* (Boevink et al., 1998; Nebenführ et al., 1999). This may reflect the different cell architecture between the densely packed cytoplasmic column of

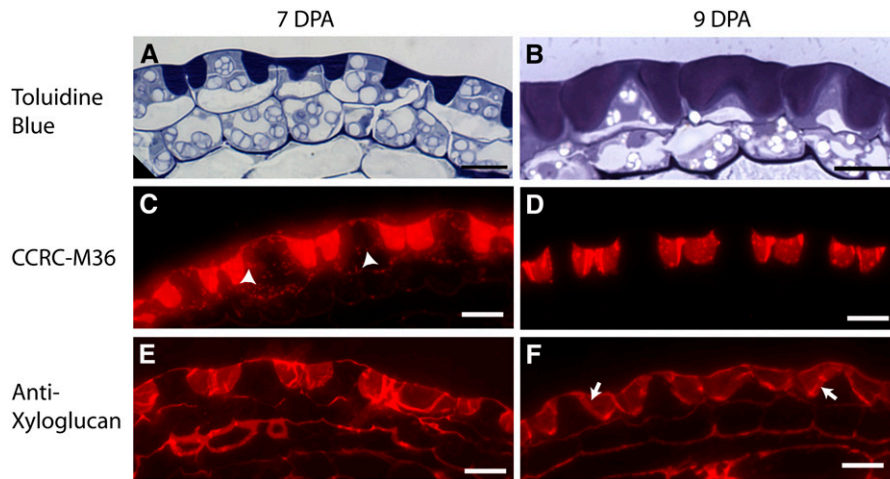


**Figure 4.** Details of Seed Mucilage (CCRC-M36) or XG ( $\alpha$ -XG) Labeling in 7- and 9-DPA Seed Coats.

(A) and (B) Toluidine blue-stained sections of cryofixed *Arabidopsis* seed coats at 7 and 9 DPA.

(C) and (D) Seed coat cells at 7 and 9 DPA showing a strong CCRC-M36 immunofluorescent label in the mucilage pocket. At 7 DPA (C), punctate structures in the cytosol also label with CCRC-M36 (arrowheads).

(E) and (F)  $\alpha$ -XG labels both the mucilage pocket and the primary cell wall. In addition,  $\alpha$ -XG labels the developing secondary cell wall of the columella (arrows) at 9 DPA (F). Wrinkles in section lead to the appearance of uneven labeling in (E).

Bars = 15  $\mu$ m.

a seed coat cell and the cortical cytoplasm of epidermal or suspension-cultured cells. The number of Golgi stacks approximately doubled from 4 DPA ( $24 \pm 9$  Golgi stacks/cell,  $n = 33$  cells; Figure 8B) to the mucilage secretion phase at 7 DPA ( $49 \pm 14$  Golgi stacks/cell,  $n = 42$  cells; Figure 8C). This was considered significant (Mann-Whitney  $U = 65.0$ ,  $P < 0.025$ ).

Together, these two techniques provide complementary information: analysis by TEM allows Golgi stacks to be positively identified, and the cytosol is sampled in square microns, providing a statistical sampling of the Golgi density. The fluorescence data can directly report the number of ST-GFP positive puncta in a whole cell. As a further comparison of two-dimensional data obtained from sections viewed by TEM and whole-cell data viewed by fluorescence microscopy, stereological techniques were used to extrapolate TEM results to whole cells (Elias and Hyde, 1983). Extrapolating on TEM results, there were  $\sim 25$  and 56 Golgi stacks per cell in 4- and 7-DPA seed coat cells, respectively, which are numbers consistent with what was found using live-cell imaging.

#### Golgi Stacks Do Not Cluster Near the Site of Secretion

Since mucilage secretion is targeted to the outer tangential side of the cell, the mobile Golgi stacks producing the secretory product theoretically could cluster at the site of secretion, eliminating much of the need for long-distance transport and targeting of vesicles to the apical domain of the plasma membrane. The distribution of Golgi stacks in the cell was compared at sites of mucilage deposition (apical region of the cell; Figure 9A) and in the portions of the cell distal to the mucilage pockets (basolateral domains; Figure 9A). Golgi stack distribution was mapped, but there were no significant differences between the

densities of Golgi stacks in the apical domain versus the basolateral domains at 7 DPA (compared using the Wilcoxon Signed-Ranks tests for repeated measures;  $z = -1.975$ ,  $P > 0.05$ ) (Figure 9B). Thus, the entire Golgi apparatus of seed coat cells is evenly distributed around the cell. This was confirmed by live-cell imaging with ST-GFP as well (Figure 8), where an even distribution of puncta in seed coat cells at 4 and 7 DPA was observed.

Although the entire population of mobile Golgi stacks does not cluster near the site of mucilage secretion, there might be a polarized distribution of mucilage-carrying Golgi in the apical region. If this were true, it would suggest that there are distinct populations of Golgi stacks (i.e., specialist Golgi stacks) that reside near the apex and produce large amounts of pectin. The distribution of the Golgi labeled with CCRC-M36 was examined using immunogold/TEM to determine whether more Golgi stacks carrying specific products were found in the areas where mucilage was incorporated. When the cellular locations of Golgi stacks containing the CCRC-M36 pectin-epitope or  $\alpha$ -XG were mapped using immunogold TEM, there were virtually no differences between the percentages of antibody gold-labeled Golgi stacks in the apical versus basolateral regions of the cells (Figure 9C). This indicates that mucilage-secreting Golgi stacks are found throughout the cell, not just in the apex, and that the majority of the Golgi stacks in the cell are involved in the production of mucilage at 7 DPA.

#### Decreased Mucilage (*mum4*) Mutants' Golgi Density Still Doubles during Mucilage Production, but Golgi Stacks Lack Elaborate TGN

The above data demonstrate that changes in Golgi number and morphology occur throughout the cell during mucilage

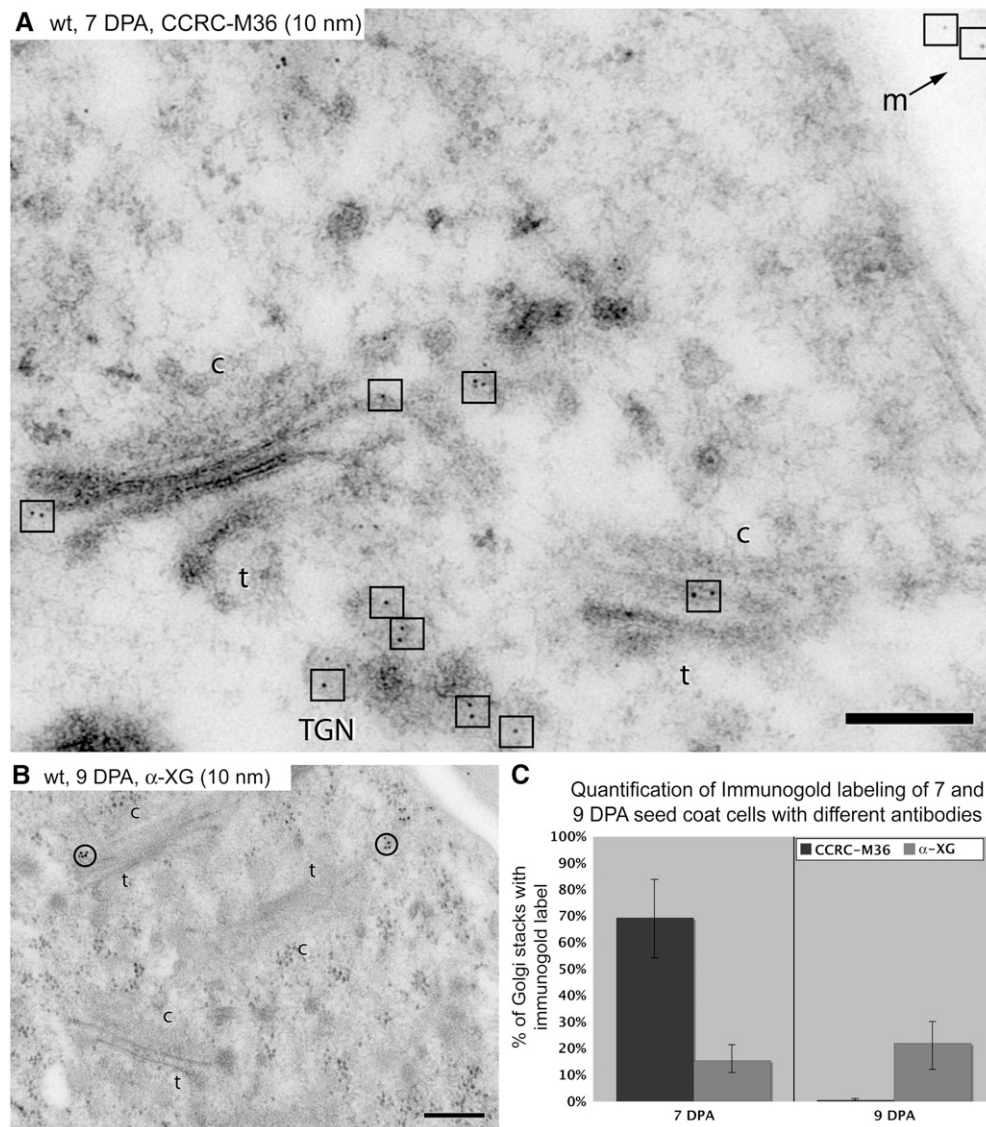


**Figure 5.** Single Epitope Immunogold Labeling of Golgi Stacks.

**(A)** Immunogold labeling of wild-type, 7-DPA seed coat cells with the antimucilage antibody, CCRC-M36, using 10-nm gold particles (squares).

**(B)** Immunogold labeling of wild-type, 9-DPA seed coat cells with  $\alpha$ -XG, using 10-nm gold particles (circles). c, *cis* face of Golgi stack; m, mucilage; t, *trans* face of Golgi stack. Bars = 250 nm.

**(C)** Percentage of Golgi stacks that immunolabel with 10-nm gold in thin sections of seed coat cells at 7 and 9 DPA. Sections were labeled with either CCRC-M36 or  $\alpha$ -XG. This analysis is based on three separate experiments, which includes a total of 31 cells and 287 Golgi stacks for 7-DPA cells labeled with CCRC-M36, 28 cells and 252 Golgi stacks for 7-DPA cells labeled with  $\alpha$ -XG, 23 cells and 287 Golgi stacks for 9-DPA cells labeled with CCRC-M36, and 20 cells and 282 Golgi stacks for 9-DPA cells labeled with  $\alpha$ -XG. Error bars represent range of percentages obtained in replicates.

production but do not determine whether the changes are in response to increases in the bulky pectin product or due to the intrinsic developmental program that seed coat cells undergo. Plants with loss-of-function mutations in *MUM4* have seed coat epidermal cells with significantly reduced amounts of mucilage (Usadel et al., 2004; Western et al., 2004; Figure 10). Comparison of the Golgi apparatus of the wild-type and *mum4* seed coat cells

at the mucilage-producing stage (7 DPA) allowed us to determine what happens to Golgi structure and numbers when the surge of pectin product is drastically reduced. As documented earlier (Figures 1D, 2, and 10B), wild-type Golgi stacks that are producing mucilage have short cisternae with compressed lumens and swollen margins as well as a convoluted TGN. In comparison, the Golgi cisternae of the stacks observed in *mum4* cells at

7 DPA were longer, with more open lumens and thin, fenestrated margins (Figure 10D). Strikingly, they had a less complex TGN, lacking the elaborate clusters of vesicles/swollen networks seen in 7-DPA wild-type cells. In this regard, the *mum4* Golgi stacks examined at 7 DPA had cisternae that were more similar in appearance to those of wild-type cells at 4 DPA (cf. Figures 1B with 10B and 10D).

The similarities and differences in Golgi morphology between the wild type and *mum4* at 7 DPA raised the question of whether the increased density (number of Golgi stacks/ $\mu\text{m}^2$ ) of Golgi stacks seen in wild-type cells between 4 and 7 DPA would also be present in *mum4*. If the production of mucilage drives Golgi proliferation, then comparison of 7-DPA wild-type and *mum4*

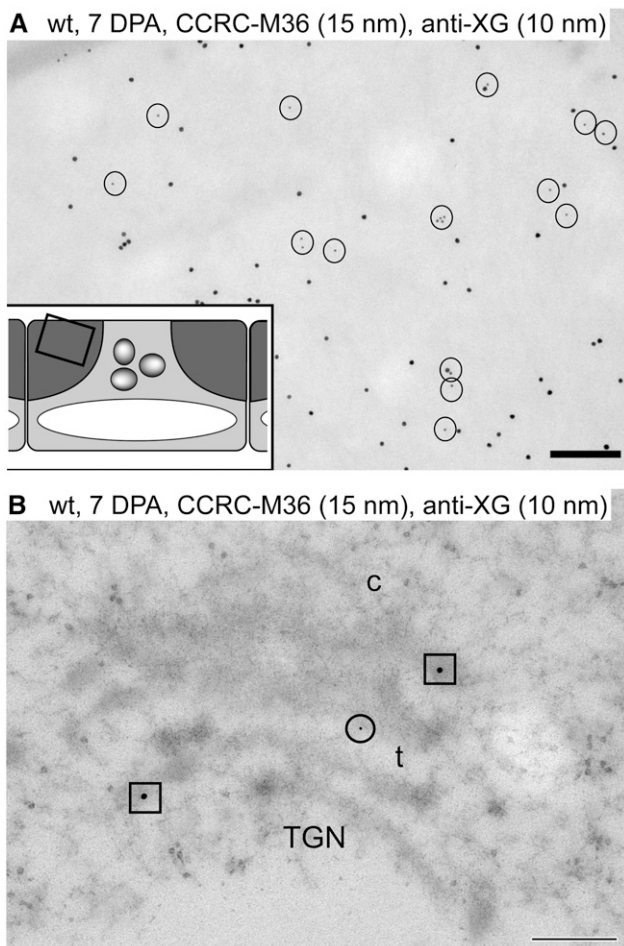


**Figure 6.** Double Immunogold Labeling of Wild-Type, 7-DPA Seed Coat Cells.

**(A)** Labeling density in seed coat mucilage within the mucilage pocket (see inset for location with respect to the seed coat cell) using CCRC-M36 (15-nm gold) and  $\alpha$ -XG (10-nm gold, circles).

**(B)** Double immunogold labeling of Golgi stack using CCRC-M36 (15-nm gold, squares) and  $\alpha$ -XG (10-nm gold, circles).

c, cis face of Golgi stack; m, mucilage; t, trans face of Golgi stack. Bar = 250 nm.

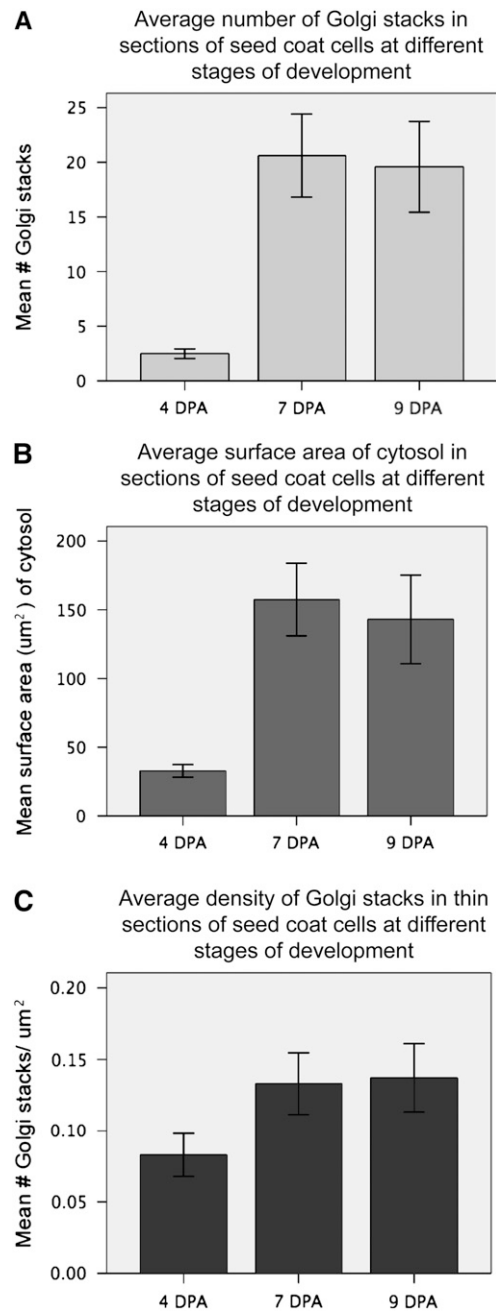


**Figure 7.** Quantification of Golgi Stacks throughout Seed Coat Development.

**(A)** Average number of Golgi stacks visible in sections of seed coat cells at 4, 7, and 9 DPA.

**(B)** Average surface area of cytosol in thin sections of seed coat cells at 4, 7, and 9 DPA. Cytosol was defined as all areas within the cytoplasm, excluding the nucleus, vacuole, and starch granules.

**(C)** Average density (number of Golgi stacks/ $\mu\text{m}^2$  cytosol) in thin sections of seed coat cells at 4, 7, and 9 DPA. For this analysis, three separate experiments were conducted, resulting in a total of 61 cells and 152 Golgi stacks at 4 DPA, 24 cells and 474 Golgi stacks at 7 DPA, and 17 cells and 333 Golgi at 9 DPA. Raw data were obtained by TEM. Error bars represent 95% confidence intervals.

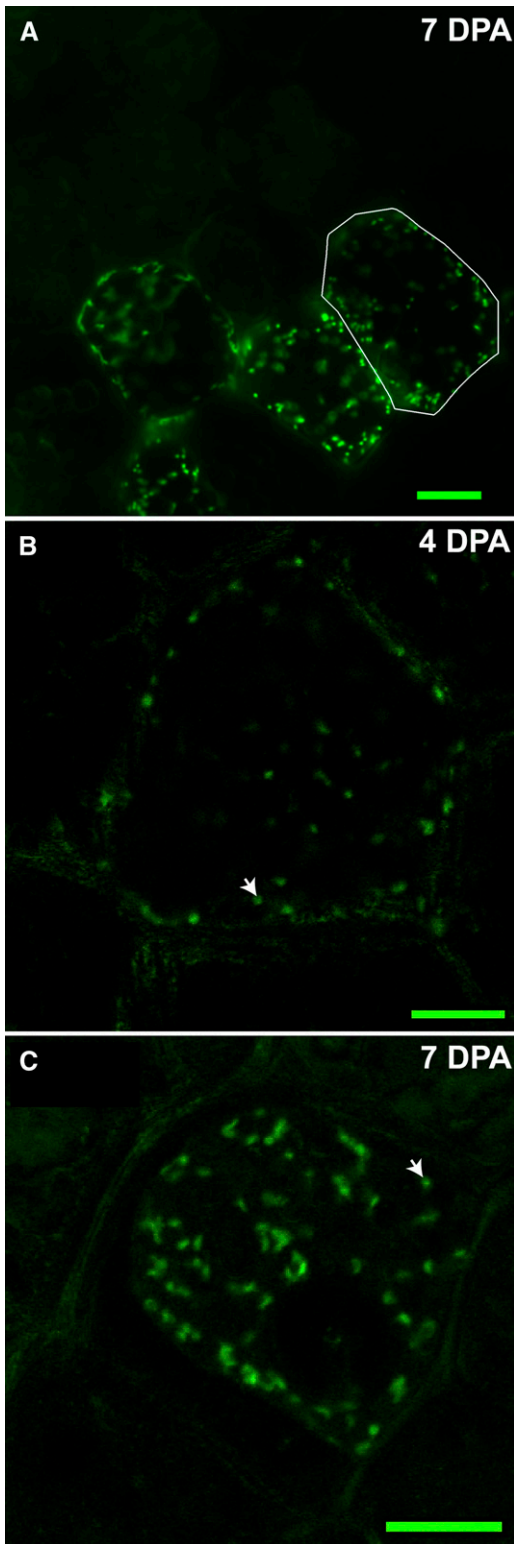


**Figure 8.** Fluorescence Microscopy Images of Wild-Type Seed Coat Cells Carrying the Golgi Marker 35S:ST-GFP.

(A) Low-magnification epifluorescence image of seed coat on whole

seed coat cells during intense mucilage production would be predicted to reveal a lower density of Golgi stacks in the *mum4* cells. By contrast, if Golgi proliferation is an intrinsic component of the development of the seed coat cells, then the *mum4* plants would be expected to display the same increases in Golgi density as the wild type during mucilage production. High-resolution electron microscopy was once again employed to examine differences in Golgi density between wild-type and *mum4* seeds at 4 or 7 DPA (Figure 11). Despite the strong reduction in the amount of mucilage produced by these cells at 7 DPA, the density of Golgi stacks in *mum4* cells at 7 DPA was not significantly different from the same developmental stage in the wild-type seed coat (Figure 11C) (Mann-Whitney U = 601.5,  $P > 0.05$ ), indicating that even with a large reduction of secretory product in the mutant, Golgi proliferation occurred between 4 and 7 DPA.

## DISCUSSION

The large increases in polysaccharide secretion in *Arabidopsis* seed coat epidermal cells are accompanied by specific changes in Golgi morphology, especially in the TGN, and a dramatic increase in Golgi number. The consistent morphological changes in the Golgi stack during mucilage secretion, as well as the identification of the pectin epitope in the majority of the Golgi stacks, imply that the individual stacks of the Golgi apparatus work synchronously to produce mucilage.

### Prolific Mucilage Production Leads to Morphological Changes in the Golgi and TGN

In this study, high levels of mucilage secretion were correlated with a specific Golgi morphology, which includes flattened cisternae with swollen, fenestrated margins and a complex TGN. From *cis* to *trans*, the cisternal lumina become increasingly flattened and the margins of the cisternae become increasingly swollen. This is consistent with what has been documented in other systems that are active in cell wall matrix production, such as root hairs (Sherrier and Vandenbosch, 1994) and mucilage-producing root cap cells (Craig and Staehelin, 1988; Staehelin et al., 1990; Mollenhauer and Morre, 1991). This correlation is further strengthened by the fact that a mutant unable to produce a high level of seed coat mucilage lacks this characteristic Golgi morphology. A hypothesis has been put forward that attempts to explain Golgi morphology in the context of biosynthetic function. Based on freeze-fracture data, it has been postulated that the bulk of the biosynthetic enzymes are maintained within the

---

seed at 7 DPA showing patchy expression of 35S:ST-GFP in the seed coat. A single cell is outlined in white.

(B) and (C) Single image taken from z-stack of a seed coat cell showing ST-GFP distribution at higher magnification at 4 and 7 DPA.

(B) Prior to mucilage production, at 4 DPA, there are fewer Golgi stacks visible (arrows).

(C) Once mucilage production is underway, at 7 DPA, there are approximately twice as many Golgi stacks in these cells.

Bars = 10  $\mu$ m.

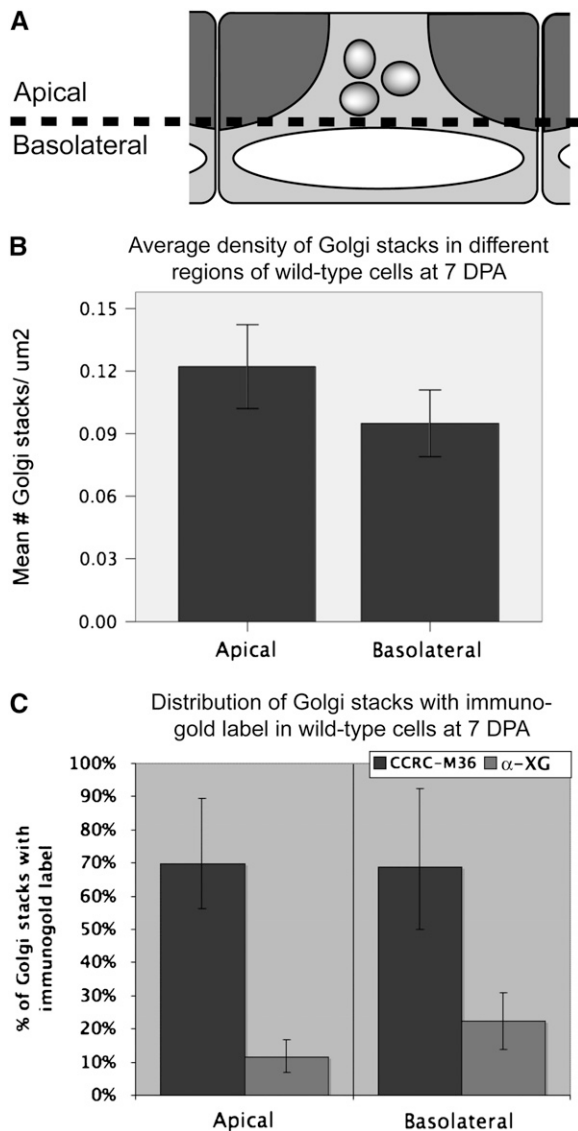


**Figure 9.** Distribution of Golgi Stacks in Wild-Type, 7-DPA Seed Coat Cells.

**(A)** Schematic representation of how the apical and basolateral regions of seed coat cells are defined.

**(B)** Comparison of the Golgi concentration in apical and basolateral regions of 7-DPA seed coat cells. This analysis was based on three separate experiments, which resulted in a total of 24 cells and 474 Golgi stacks being examined. Error bars represent 95% confidence intervals. Differences were not considered significant ( $P > 0.05$ ).

**(C)** Comparison of regions of 7-DPA cells that label with immunogold (anti-mucilage (CCRC-M36) or  $\alpha$ -XG), indicating an even distribution of epitopes in all regions of the cell. For this analysis, a total of 31 cells and 287 Golgi stacks using CCRC-M36, and 28 cells and 252 Golgi stacks using  $\alpha$ -XG were examined, in three separate experiments. Error bars represent the range of percentages obtained in different replicates.

flattened central portion of the Golgi stack, while the nascent polysaccharide chains are pushed outwards, forming the swollen margins of the cisternae, and concentrating the polysaccharide product for vesicle transport (Staehelein et al., 1990). If this model is correct, the decreased amount of mucilage that is being produced in *mum4* would explain why the margins of cisternae do not appear swollen and the TGN is decreased. It would be interesting to examine if *mum4* Golgi stacks show similar results to the wild type in freeze fracture, which would imply that the amount of biosynthetic enzymes embedded within the cisternae are similar.

During mucilage production, RGI-rich pectin is produced in large amounts by the Golgi and must be packaged at the *trans*-face of the Golgi stack. Tomography and immunogold labeling demonstrated that the Golgi exit site for pectins at the TGN consists of interconnected vesicular clusters filled with pectin product. That this exit site is a network, rather than free vesicles, suggests that there must be subsequent fission and/or budding steps to give rise to free secretory vesicles. The clustered vesicles of the TGN appear to mature into dense secretory vesicles, which move to the cortical cytoplasm, where they can be observed among the abundant microtubules lining the mucilage secretion domain (McFarlane et al., 2008). This is unlike the peripheral root cap cells' mucilage secretion, where large bulbous margins of the Golgi stacks become large secretory vesicles after a process of clathrin-coated membrane retrieval (Mollenhauer and Morre, 1991).

In this system, mutant analyses and antimucilage antibody labeling data demonstrate the importance of the TGN in anterograde transport of cell wall materials. The TGN appeared in close association with Golgi stacks in this study, which was also the case in electron tomographic examinations of entire *Arabidopsis* meristematic cells at all stages of the cell cycle (Segui-Simarro and Staehelein, 2006). In another polarized secretory system, RabA4b has been reported to be a marker of a unique post-TGN compartment that is localized in the secretory zone of root hairs during tip growth (Preuss et al., 2004, 2006; Thole et al., 2008). With the emphasis on cargo that was used in our study, a similar post-Golgi compartment could not be confirmed, but the existence of a compartment that could mediate vesicle production and/or membrane recycling is entirely possible. The TGN itself has been proposed to be a site where multiple anterograde (secretion and vacuolar protein sorting) and retrograde (endocytic) pathways converge (reviewed in Lam et al., 2007).

### Biological Control of Golgi Proliferation

The upregulation of pectin synthesis for the production of mucilage in the seed coat epidermis occurs prior to 7 DPA and is correlated with a dramatic increase in the number of Golgi stacks. In *mum4*, both the size and timing of the increase in Golgi density remain unchanged, even though the production of mucilage is dramatically reduced. Although polysaccharide secretion required for the formation of the columella still occurs (at 9 DPA), it is not correlated in time with the increase in Golgi density. The fact that the timing of the proliferation of Golgi stacks in the *mum4* mutant is identical to the wild type, despite a dramatic reduction in the secretory demands on the *mum4* cell, implies

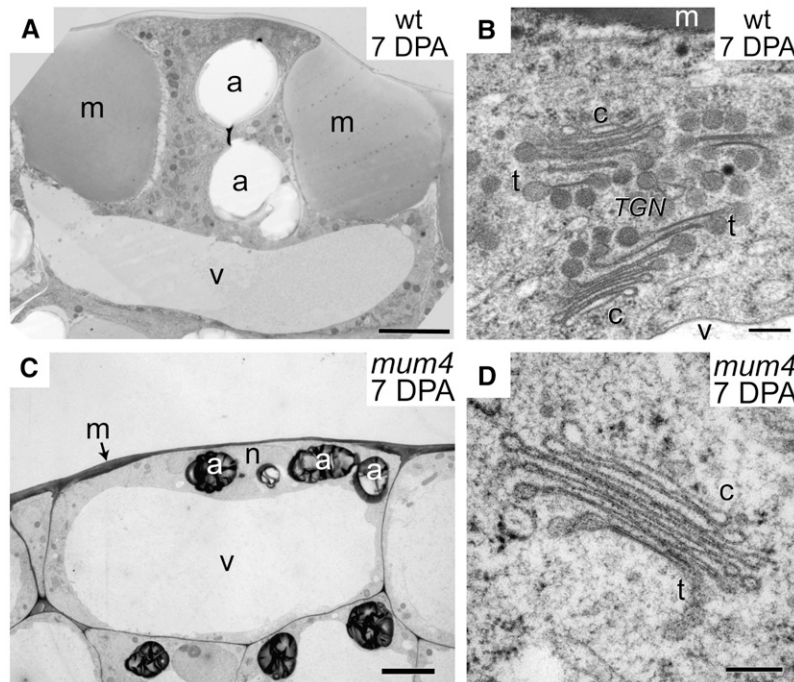


**Figure 10.** Comparison of Wild-Type and *mum4* Seed Coat Cell Morphology and Golgi Ultrastructure at 7 DPA.

**(A)** A wild-type, 7-DPA seed coat cell. Note the large mucilage pocket and central cytoplasmic column, with starch granules in amyloplasts above the vacuole.

**(B)** Close-up of a 7-DPA Golgi stack.

**(C)** A *mum4* seed coat cell at 7 DPA. Cells are flatter than wild-type cells, with very small mucilage pockets and virtually no central cytoplasmic column. Vacuoles are approximately the same size in both wild-type and *mum4* cells.

**(D)** Close-up of *mum4* Golgi stack.

a, amyloplast; c, cis face of Golgi stack; m, mucilage; n, nucleus; t, trans face of Golgi stack; V, vacuole. Bars = 5  $\mu\text{m}$  in **(A)** and **(C)** and 250 nm in **(B)** and **(D)**.

that Golgi proliferation is not a direct consequence of polysaccharide production. Instead, Golgi proliferation may be independently activated by developmental signals during cell differentiation. The nature of such developmental signals has yet to be elucidated. The mechanism of Golgi doubling in these cells is also not known, but, in plants, Golgi fission is considered to be the mostly likely mechanism (Bosabalidis, 1985; Craig and Staehelin, 1988; Hirose and Komamine, 1989; Langhans et al., 2007). However, de novo production of Golgi stacks (Langhans et al., 2007) could be involved as well.

#### Golgi Stacks Respond Synchronously and Collectively Represent a Single Golgi Apparatus

Current views of cell wall architecture, based on antibody localization, postulate that cell wall domains with distinct epitopes are laid down during development (Knox, 1997). In the past, this has raised the question of what proportion of the hundreds of streaming stacks in the plant Golgi apparatus contribute to a particular epitope's production and secretion. The detection of RGI epitopes in seed coat cells, as recognized by the CCRC-M36 monoclonal antibody, allowed us to test this question. Both the uniform morphological changes of the Golgi stacks and the high

proportion of stacks that colocalize with CCRC-M36 label support the view that production of mucilage occurs synchronously in the vast majority of stacks in the Golgi apparatus.

#### Dispersed Production of Matrix Polysaccharides by Golgi Stacks for Polarized Secretion

During the development of the *Arabidopsis* seed coat, the targeted secretion of matrix polysaccharides is not accompanied by a concentration of Golgi stacks near the site of cargo deposition. This indicates that the clustering of Golgi stacks is not a mechanism for the proper targeting of cell wall carbohydrates to their destination in the developing mucilage pocket. The dispersed Golgi stacks observed in this study are contrary to the situation observed in other plant cells where polarized growth has been observed. In root hairs (Sherrier and Vandenbosch, 1994) and trichomes (Lu et al., 2005) and in cell plate formation during cytokinesis (Nebenführ et al., 2000; Segui-Simarro and Staehelin, 2006), targeted secretion of cell wall products is accompanied by a clustering of Golgi in the region of the cell where deposition is high. In the case of cell plate formation, the overall density of Golgi stacks in meristematic root cells remains relatively constant despite local increases in the number of Golgi

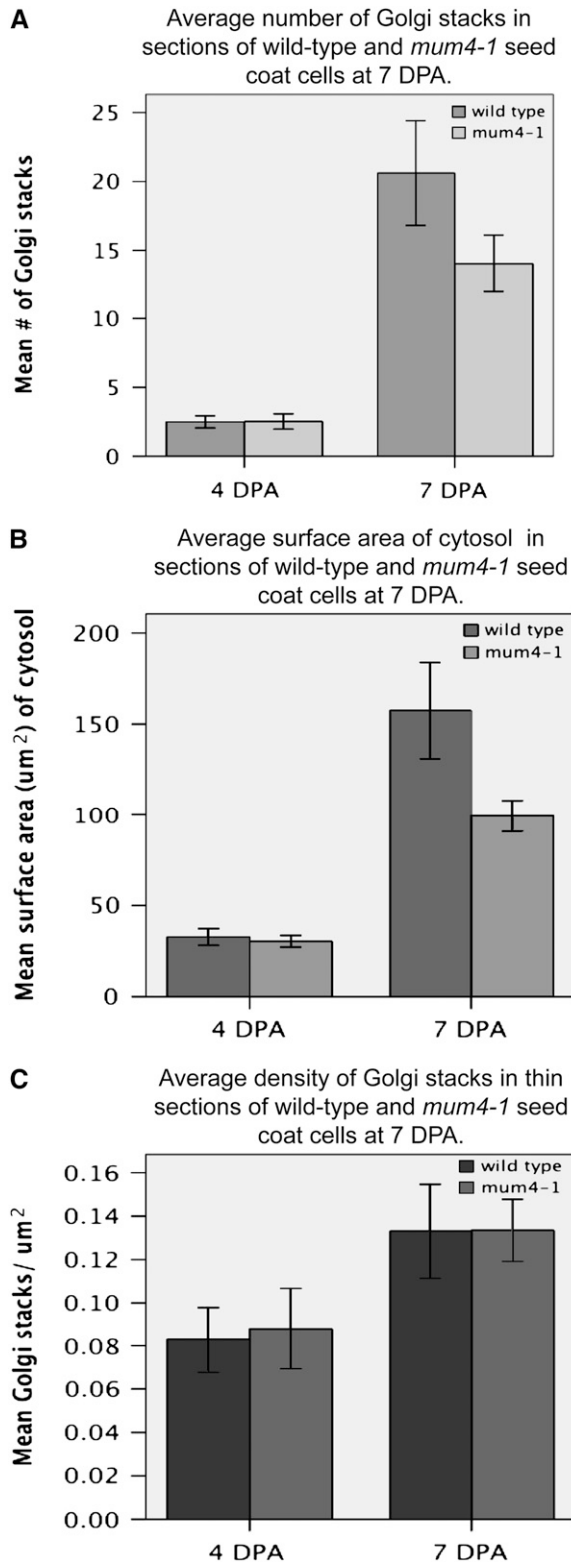


**Figure 11.** Quantification of Changes in Golgi Stacks in Wild-Type and *mum4* Seed Coat Cells at 4 and 7 DPA.

**(A)** Comparison of the average number of Golgi stacks visible in thin sections of wild-type and *mum4* seed coat cells.

stacks near the cell plate (Segui-Simarro and Staehelin, 2006). The nonpolarized distribution of Golgi stacks seen here is more similar to the arrangement in expanding interphase plant cells (Boevink et al., 1998; Segui-Simarro and Staehelin, 2006), especially in mucilage-secreting root cap cells (Staehelin et al., 1990). However, even in such cases of diffuse growth, there is evidence of targeted secretion of macromolecules to specific wall domains, as seen in the case of COBRA in the periclinal walls of the root (Roudier et al., 2005).

If the Golgi stacks are dispersed, yet specifically deposit pectins and other matrix components at the mucilage pocket, then post-Golgi mechanisms for vesicle targeting must be acting to ensure that cell wall products are targeted to the appropriate domain of the plasma membrane. Plant homologs of the molecular machinery involved in this process in other eukaryotes have been identified *in silico* (Jürgens and Geldner, 2002), but their exact roles in plants have not been determined in many cases. The major plasma membrane targeting complex in yeast and animals is the exocyst (Guo et al., 2000), an eight-protein complex that most likely forms a rod-like structure to facilitate docking of the incoming vesicles at the target membrane (Munson and Novick, 2006). All eight subunits have been identified in *Arabidopsis*, and there is some evidence that three of the subunits, RTH1/SEC3 (Wen and Schnable, 1994; Wen et al., 2005), SEC8 (Cole et al., 2005), and EXO70 (Elias et al., 2003; Synek et al., 2006), play a role in targeting vesicles to the plasma membrane. In mutant analyses of these three subunits, targeted secretion appears to be disrupted, resulting in decreased ability of certain cells, such as root hairs or pollen tubes, to elongate. However, the phenotype of impaired secretion of seed coat mucilage in these mutants, as well as in those of other exocyst mutants, has not been determined.

#### XG in the Mucilage and the Columella

Our data demonstrate that both the mucilage and the columella of the seed coat label with antibodies for XG. Considering that XG is usually associated with the network of primary cell wall cellulose microfibrils and that cellulose has been found to be a component of mucilage in the *Arabidopsis* seed coat (see Supplemental Figure 1 online; Willats et al., 2001a; Macquet et al., 2007), the presence of XG in the mucilage is not surprising.

On the other hand, the columella is considered to be a secondary cell wall by definition, due to the fact that it is laid down after the completion of cell expansion. XG is the hemicellulose most commonly associated with type I primary cell walls

**(B)** Average surface area of cytosol in thin sections wild-type and *mum4* seed coat cells.

**(C)** Average density (number of Golgi stacks/ $\mu\text{m}^2$  cytosol) in thin sections of 7-DPA wild-type and *mum4* seed coat cells. For this analysis, three separate experiments were conducted. For the wild type, a total of 61 cells and 152 Golgi stacks at 4 DPA and 24 cells with 474 Golgi stacks at 7 DPA were examined. In the case of *mum4*, 46 cells and 115 Golgi stacks were examined at 4 DPA and 57 cells with 800 Golgi stacks were examined at 7 DPA. In all cases, data were acquired using TEM. Error bars represent 95% confidence intervals.

(Carpita and Gibeaut, 1993), whereas secondary cell walls in other cell types of *Arabidopsis*, such as xylem and interfascicular fibers, show reactivity with antixylan antibodies (such as LM10 and LM11) (McCartney et al., 2005; Persson et al., 2007). In developing hybrid aspen (*Populus tremula* × *P. tremuloides*) secondary xylem, fucosylated XGs were localized with CCRC-M1 to the compound middle lamella region of the secondary cell wall of fibers and are believed to link the primary and secondary cell walls during secondary cell wall deposition (Bourquin et al., 2002). Therefore, the presence of XG throughout the secondary cell wall layer in the seed coat is intriguing.

### Tracking Polysaccharide Production with Mucilage-Specific Antibodies

We have shown that the CCRC-M36 antibody reacts only with mucilage in the developing seed, providing an invaluable tool for the analysis of seed coat mucilage secretion. Although there are other antibodies that label seed coat mucilage, including  $\alpha$ -XG (reported here) and PGA/RGI (Western et al., 2004), CCRC-M36 has the advantage that it is specific to mucilage, rather than primary cell wall, in the *Arabidopsis* seed coat. This fact has allowed us to selectively track cargo that is being targeted to a specific cell wall domain. Thus far, we have been able to show that Golgi stacks carrying cargo destined for polar secretion do not cluster near the target site but are instead evenly distributed throughout the cell. Future experiments made possible with this antibody include examining how polysaccharides and enzymatic cargo destined for the apoplast are packaged and sorted by the Golgi apparatus and the screening for mutants in which mucilage has been mislocalized to other areas of the seed coat's apoplast.

## METHODS

### Plant Materials and Growth Conditions

Wild-type *Arabidopsis thaliana* was Columbia-2 ecotype (Lehle Seeds). The mutant line *mum4-1* (here referred to as *mum4*) was isolated in Western et al. (2001). Seeds were grown on prepared soil mix (Sunshine 5 Professional Growing Mix; Sungro Horticulture Canada) that had been fertilized with AT media (Haughn and Somerville, 1986) in growth chambers at 21°C under continuous light (90 to 120  $\mu\text{E m}^{-2}\text{s}^{-1}$  PAR). Flowers were initially staged as by Western et al. (2000). In addition, stages were defined by the morphology of seed coat cells upon examination at the light microscopy level (see below).

### High-Pressure Freezing and Freeze Substitution

Seeds 4, 7, and 9 DPA (Western et al., 2004) were excised from siliques, stabbed with an insect pin (in the case of 7- and 9-DPA seeds), and prepared for TEM by high-pressure freezing, freeze substitution, and resin embedding according to Rensing et al. (2002). Briefly, samples were loaded into copper hats (Ted Pella) filled with 1-hexadecene and high-pressure frozen using a Bal-Tec HPM 010 high-pressure freezer (Balzers Instruments). The hats were immediately transferred to frozen cryovials containing freeze substitution medium consisting of either 2% (w/v) osmium tetroxide in acetone with 8% (v/v) dimethoxypropane for morphological assays or 0.25% (v/v) glutaraldehyde and 2% (w/v) uranyl acetate in acetone with 8% (v/v) dimethoxypropane for immunolabeling assays. Freeze substitution was performed for 4 to 6 d at  $-80^\circ\text{C}$  by

incubation in an acetone/dry ice slush, followed by transfer of the cryovials into a metal block precooled to  $-20^\circ\text{C}$ , which was warmed over 20 h to allow reaction of fixatives. The samples were removed from the sample holders, rinsed in anhydrous acetone several times, and slowly infiltrated and embedded in either Spurr's resin (Spurr, 1969) for morphological examination or LR White (London Resin Company) for immunological studies.

### Morphological Assays

Thick (0.5  $\mu\text{m}$ ) sections, stained with toluidine blue, were examined by light microscopy for intact seed coat cells at each stage of development and to ensure that embedded seeds had seed coats at the appropriate developmental stage, based on morphological criteria described previously (Western et al., 2000). Samples containing appropriately staged seeds were thin sectioned using a Leica Ultracut UCT (Leica Microsystems) and mounted on 150 mesh Formvar-coated grids. Sections were poststained with 2% (w/v) aqueous uranyl acetate in 70% (v/v) methanol (for 10 min) and Reynold's lead citrate (for 5 min). Samples were examined using a Hitachi H-7600 PC-TEM microscope.

To calculate the density of Golgi in thin sections (number of Golgi stacks/ $\mu\text{m}^2$  cytosol), the number of Golgi stacks visible in a given TEM section of a cell was counted, and images of the counted cells were collected. The cytosol was defined as all areas within the cytoplasm, except the nucleus, amyloplasts, and vacuole. The surface area of the cytosol was calculated using ImageJ (National Institutes of Health; <http://rsb.info.nih.gov/ij/>). The number of cells measured was chosen so that there were approximately equivalent amounts of cytosolic surface area measured at all 3-d stages. This resulted in the examination of a total of 61 wild-type cells and 152 Golgi stacks at 4 DPA, 24 cells and 474 Golgi stacks at 7 DPA, and 17 cells and 333 Golgi at 9 DPA. In the case of *mum4*, 46 cells and 115 Golgi stacks were examined at 4 DPA and 57 cells with 800 Golgi stacks at 7 DPA. Extrapolation of stack density in sectioned material to stack density in whole cells was done according to Elias and Hyde (1983).

### Live-Cell Imaging of Golgi Stacks

Seeds from transgenic plants bearing the *trans*-Golgi marker ST-GFP, driven by the 35S promoter (35S:ST-GFP) (Boevink et al., 1998) were staged, removed from siliques, and mounted in SlowFade Antifade reagent (Invitrogen). Samples were visualized by obtaining z-stacks of entire cells using a Zeiss LSM510 Meta confocal microscope (Carl Zeiss Canada) or by epifluorescence of whole cells using a Leica DM6000B microscope with fluorescent source (Leica Microsystems) at  $\times 63$  magnification immediately after the seeds were removed from siliques. ImageJ software was used to identify and count Golgi-sized punctate structures in individual seed coat cells. Thirty-three 4-DPA cells were counted, with a total of 776 Golgi stacks, whereas 42 cells were counted at 7 DPA, yielding 2070 Golgi stacks.

### Primary Antibodies

Previously published antibodies that were used include JIM5 and JIM7 against methyl-esterified homogalacturonans (Knox et al., 1990),  $\alpha$ -RGI/PGA against rhamnogalacturonan/polygalacturonic acids,  $\alpha$ -XG against XG (Moore et al., 1986), PAM1 against unesterified homogalacturonans (Willats et al., 1999), LM5 against anti-(1-4)- $\beta$ -D-galactan (Jones et al., 1997), LM7 against partially methylesterified homogalacturonan (Willats et al., 2001b), LM10 against xylans (McCartney et al., 2005), CBD-OG (McLean et al., 2000), CCRC-M1 against fucosylated XG, and CCRC-M2 and CCRC-M7 against RGI (Puhlmann et al., 1994). Another set of antibodies used (CCRC-M30, CCRC-M31, CCRC-M32, CCRC-M34, CCRC-M36, and CCRC-M38) was generated against extracted *Arabidopsis*

seed mucilage (T. Bootten, Z. Popper, C. Deng, R. Jia, W.S. York, M.A. O'Neill, and M.G. Hahn, unpublished data), and these antibodies are available from CarboSource ([http://cell.ccrcc.uga.edu/~carbosource/CSS\\_home.html](http://cell.ccrcc.uga.edu/~carbosource/CSS_home.html)). A further set of antibodies (CCRC-M48, CCRC-M54, CCRC-M57, and CCRC-M58) was generated against tamarind seed XG (Z. Popper, T. Bootten, S. Tuomivaara, A.G. Swennes, R. Jia, W.S. York, and M.G. Hahn, unpublished data), and these antibodies are also available from CarboSource.

### Immunofluorescence

For immunofluorescence, 0.3- to 0.5- $\mu$ m LR White sections were mounted on 10-well, Teflon-coated microscope slides. Nonspecific protein binding was blocked by incubating slides in Coplin jars filled with 5% (w/v) nonfat dry milk (NFD) in Tris-buffered saline/0.1% (v/v) Tween 20 (TBST) for 20 min. Samples were then incubated at room temperature for 1 h with primary antibodies at 1:20 (v/v) dilutions in 1% (w/v) NFD in TBST and for 1 h in secondary antibodies at 1:100 (v/v) dilution. Control experiments were performed to test specific binding of primary antibodies in CCRC-M36 and  $\alpha$ -XG label experiments by preincubating the antibodies with their specific purified antigen to block antibody binding sites. Antigen for CCRC-M36 was mucilage that had been extracted from wild-type seeds by vortexing whole seeds, and the antigen for anti-XG was 2 mg/mL of tamarind XG (Megazyme International Ireland). In both cases, preincubation of primary antibody with excess antigen completely blocked binding to the sections (see Supplemental Figure 2 online). Rinses were performed before and after incubations in Coplin jars with TBST. Samples were mounted in 90% (v/v) glycerol in water and examined via epifluorescence using a Leica DMR light microscope (Leica Microsystems). For whole seed immunolabeling (see Supplemental Figure 1 online), we followed the same protocol, except that incubations were done in small batches (10 to 50) of whole seeds, in 1.5-mL microcentrifuge tubes with gentle agitation on an orbital shaker.

### Immunogold Labeling

LR White samples were cut into 70-nm sections and mounted on 200 mesh, fine bar, nickel grids (Ted Pella). Nonspecific protein binding was blocked with 5% (w/v) NFD in TBST for 20 min. Excess solution was blotted off, and grids were transferred to a drop of primary antibody, diluted 1:5 (CCRC-M36) or 1:20 ( $\alpha$ -XG) with 1% (w/v) NFD in TBST, and incubated for 1 h at room temperature. After washing grids in three subsequent washes of TBST for 15 s each, grids were transferred to secondary antibodies and diluted 1:100 with 1% (v/v) NFD in TBST for 1 h. Secondary antibodies were goat anti-mouse IgG + IgM (for CCRC-M36) or goat anti-rabbit IgG (for  $\alpha$ -XG), conjugated to 10-nm colloidal gold (Ted Pella). Grids were washed again, followed by three washes of distilled water for 15 s each, and then poststained with 2% (w/v) uranyl acetate for 8 min and Reynold's lead citrate for 2 min. For the double label (i.e., CCRC-M36 and  $\alpha$ -XG), 15-nm colloidal gold conjugated to goat anti-mouse IgG + IgM was used to locate CCRC-M36. Primary or secondary antibodies were mixed together and treated as described above. Labeled Golgi stacks were counted manually. Total counts were 31 cells and 287 Golgi stacks for 7-DPA cells labeled with CCRC-M36, 28 cells and 252 Golgi stacks for 7-DPA cells labeled with  $\alpha$ -XG, 23 cells and 287 Golgi stacks for 9-DPA cells labeled with CCRC-M36, and 20 cells and 282 Golgi stacks for 9-DPA cells labeled with  $\alpha$ -XG. For the double label, 57 Golgi stacks were examined in five different cells.

### Statistical Analysis

Data analysis was conducted with SPSS 13 software. Since the data failed the Kolmogorov-Smirnov test for normalcy, nonparametric tests

were used. For comparison of three independent samples (i.e., 4, 7, and 9 DPA), significance was analyzed using the Kruskal-Wallis test (H) to compare multiple means, followed by the Mann-Whitney test (U) as a post hoc test, taking into account Bonferroni's correction for significance levels. When there were two independent samples, a Mann-Whitney test (U) was performed. For repeated measures on the same sample (e.g., apical versus basolateral calculations), a Wilcoxon signed ranks test (reported as a z-score) was used. In all cases, results were deemed significant if  $P < 0.05$ .

### Electron Microscopy Tomography

Tomographic analysis of 7-DPA seed coat cells was done according to Donohoe et al. (2006), with some minor changes. Briefly, samples were cryofixed and embedded as described above. Spurr's sections (200 nm thick) were picked up on 0.75% (w/v) Formvar-coated copper/rhodium slot grids and stained with 2% (w/v) uranyl acetate in 70% (v/v) methanol for 20 to 25 min, followed by Reynold's lead citrate for 6 to 8 min. After staining, 15-nm unconjugated colloidal gold particles were added to both sides of the grid to be used as fiducial markers to align the series of tilted images.

Tomograms were acquired on an FEI Technai TF30 intermediate voltage electron microscope, operating at 300 kV. Tilt series were acquired at 23,000 $\times$ , from  $-60^\circ$  to  $+60^\circ$  at  $1^\circ$  intervals about two orthogonal axes (Mastrorade, 1997) using a Gatan Megascan 795 digital camera, giving a calculated pixel size of 1 nm. Dual-axis tomograms were generated using the Etomo software interface, a part of the IMOD software package (Kremer et al., 1996). Tomograms were displayed and analyzed with 3dmod, the graphics component of the IMOD software package. Golgi stacks, vesicles, and other structures were modeled manually according to Donohoe et al. (2006).

### Accession Numbers

Arabidopsis Genome Initiative codes are At1g53500 (MUM4) and CS3907 (*mum4-1*).

### Supplemental Data

The following materials are available in the online version of this article.

**Supplemental Figure 1.** Antibody Screen of Mucilage from Hydrated Mature Seeds.

**Supplemental Figure 2.** Fluorescent Labeling Antibody Controls.

### ACKNOWLEDGMENTS

We thank Andrew Staehelin (University of Colorado, Boulder, CO) for constructive criticism of the manuscript and Zach Gergely (University of Colorado) and the staff of the Boulder Lab for three-dimensional electron microscopy of cells for invaluable help with tomography. The assistance of the staff of the University of British Columbia Bioluminescence Facility (Vancouver, Canada) is gratefully acknowledged. We also thank David Bird (University of Winnipeg, Winnipeg, Canada) for insightful discussion on statistics. CBD-OG was a generous gift from Douglas Kilburn (Michael Smith Laboratories, University of British Columbia, Vancouver, Canada). This work was supported by the National Science and Engineering Research Council of Canada Discovery Grants to G.W.H., T.L.W., and A.L.S. Generation and characterization of the monoclonal antibodies against plant cell wall polysaccharides was supported by a grant (DCB-0421683) from the U.S. National Science Foundation Plant Genome Program (to M.G.H.).

Received February 15, 2008; revised April 5, 2008; accepted May 16, 2008; published June 3, 2008.

## REFERENCES

- Beeckman, T., De Rycke, R., Viane, R., and Inze, D.** (2000). Histological study of seed coat development in *Arabidopsis thaliana*. *J. Plant Res.* **113**: 139–148.
- Boevink, P., Oparka, K., Santa Cruz, S., Martin, B., Betteridge, A., and Hawes, C.** (1998). Stacks on tracks: The plant Golgi apparatus traffics on an actin/ER network. *Plant J.* **15**: 441–447.
- Bosabalidis, A.M.** (1985). A possible new mode of dictyosome duplication in plant cells. *Tissue Cell* **17**: 279–286.
- Bourquin, V., Nishikubo, N., Abe, H., Brumer, H., Denman, S., Eklund, M., Christiernin, M., Teeri, T.T., Sundberg, B., and Mellerowicz, E.J.** (2002). Xyloglucan endotransglycosylases have a function during the formation of secondary cell walls of vascular tissues. *Plant Cell* **14**: 3073–3088.
- Carpita, N.C., and Gibeaut, D.M.** (1993). Structural models of primary cell walls in flowering plants: Consistency of molecular structure with the physical properties of the walls during growth. *Plant J.* **3**: 1–30.
- Carpita, N.C., and McCann, M.C.** (2000). The Cell Wall. In *Biochemistry and Molecular Biology of Plants*, B.B. Buchanan, W. Gruissem, and R.L. Jones, eds (Rockville, MD: American Society of Plant Physiologists), pp. 52–109.
- Cole, R.A., Synek, L., Zarsky, V., and Fowler, J.E.** (2005). SEC8, a subunit of the putative Arabidopsis exocyst complex, facilitates pollen germination and competitive pollen tube growth. *Plant Physiol.* **138**: 2005–2018.
- Cosgrove, D.J.** (2005). Growth of the plant cell wall. *Nat. Rev. Mol. Cell Biol.* **6**: 850–861.
- Craig, S., and Staehelin, L.A.** (1988). High pressure freezing of intact plant tissues evaluation and characterization of novel features of the endoplasmic reticulum and associated membrane systems. *Eur. J. Cell Biol.* **46**: 80–93.
- Doblin, M.S., Vergara, C.E., Read, S., Newbigin, E., and Bacic, A.** (2003). The plant cell wall: Making the bricks. In *The Plant Cell Wall*, J.K.C. Rose, ed (Oxford, UK: Blackwell Publishing), pp. 183–222.
- Donohoe, B.S., Mogelsvang, S., and Staehelin, L.A.** (2006). Electron tomography of ER, Golgi and related membrane systems. *Methods* **39**: 154–162.
- Elias, H., and Hyde, D.M.** (1983). *A Guide to Practical Stereology*. (Basel, Switzerland: S. Karger AG).
- Elias, M., Drdova, E., Ziak, D., Bavlnka, B., Hala, M., Cvrckova, F., Soukupova, H., and Zarsky, V.** (2003). The exocyst complex in plants. *Cell Biol. Int.* **27**: 199–201.
- Griffing, L.R.** (1991). Comparisons of Golgi structure and dynamics in plant and animal cells. *J. Electron Microsc. Tech.* **17**: 179–199.
- Guo, W., Sacher, M., Barrowman, J., Ferro-Novick, S., and Novick, P.** (2000). Protein complexes in transport vesicle targeting. *Trends Cell Biol.* **10**: 251–255.
- Haughn, G.W., and Somerville, C.** (1986). Sulfonylurea-resistant mutants of *Arabidopsis thaliana*. *Mol. Gen. Genet.* **204**: 430–434.
- Hirose, S., and Komamine, A.** (1989). Changes in ultrastructure of Golgi apparatus during the cell cycle in a synchronous culture of *Catharanthus roseus*. *New Phytol.* **111**: 599–605.
- Jarvis, M.C., and McCann, M.C.** (2000). Macromolecular biophysics of the plant cell wall: Concepts and methodology. *Plant Physiol. Biochem.* **38**: 1–13.
- Jones, L., Seymour, G.B., and Knox, J.P.** (1997). Localization of pectic galactan in tomato cell walls using a monoclonal antibody specific to [1->4]-[beta]-D-galactan. *Plant Physiol.* **113**: 1405–1412.
- Jürgens, G.** (2005). Cytokinesis in higher plants. *Annu. Rev. Plant Biol.* **56**: 281–299.
- Jürgens, G., and Geldner, N.** (2002). Protein secretion in plants: From the trans-Golgi network to the outer space. *Traffic* **3**: 605–613.
- Knox, J.P.** (1997). The use of antibodies to study the architecture and developmental regulation of plant cell walls. *Int. Rev. Cytol.* **171**: 79–120.
- Knox, J.P., Linstead, P.J., King, J., Cooper, C., and Roberts, K.** (1990). Pectin esterification is spatially regulated both within cell walls and between developing tissues of root apices. *Planta* **181**: 512–521.
- Kremer, J.R., Mastronarde, D.N., and McIntosh, J.R.** (1996). Computer visualization of three-dimensional image data using IMOD. *J. Struct. Biol.* **116**: 71–76.
- Lam, S.K., Tse, Y.C., Robinson, D.G., and Jiang, L.** (2007). Tracking down the elusive early endosome. *Trends Plant Sci.* **12**: 497–505.
- Langhans, M., Hawes, C., Hillmer, S., Hummel, E., and Robinson, D.G.** (2007). Golgi regeneration after brefeldin A treatment in BY-2 cells entails stack enlargement and cisternal growth followed by division. *Plant Physiol.* **145**: 527–538.
- Lu, L., Lee, Y.R., Pan, R., Maloof, J.N., and Liu, B.** (2005). An internal motor kinesin is associated with the Golgi apparatus and plays a role in trichome morphogenesis in Arabidopsis. *Mol. Biol. Cell* **16**: 811–823.
- Lynch, M.A., and Staehelin, L.A.** (1992). Domain-specific and cell type-specific localization of two types of cell wall matrix polysaccharides in the clover root tip. *J. Cell Biol.* **118**: 467–479.
- Macquet, A., Ralet, M.-C., Kronenberger, J., Marion-Poll, A., and North, H.M.** (2007). In situ, chemical and macromolecular study of the composition of *Arabidopsis thaliana* seed coat mucilage. *Plant Cell Physiol.* **48**: 984–999.
- Mastronarde, D.N.** (1997). Dual-axis tomography: An approach with alignment methods that preserve resolution. *J. Struct. Biol.* **120**: 343–352.
- McCartney, L., Marcus, S.E., and Knox, J.P.** (2005). Monoclonal antibodies to plant cell wall xylans and arabinoxylans. *J. Histochem. Cytochem.* **53**: 543–546.
- McFarlane, H.E., Young, R.E., Wasteneys, G.O., and Samuels, A.L.** (2008). Cortical microtubules mark the mucilage secretion domain of the plasma membrane in Arabidopsis seed coat cells. *Planta* **227**: 1363–1375.
- McLean, B.W., Bray, M.R., Boraston, A.B., Gilkes, N.R., Haynes, C.A., and Kilburn, D.G.** (2000). Analysis of binding of the family 2a carbohydrate-binding module from *Cellulomonas fimi* xylanase 10A to cellulose: Specificity and identification of functionally important amino acid residues. *Protein Eng.* **13**: 801–809.
- Mollenhauer, H.H., and Morre, D.J.** (1991). Perspectives on Golgi apparatus form and function. *J. Electron Microsc. Tech.* **17**: 2–14.
- Moore, P.J., Darvill, A.G., Albersheim, P., and Staehelin, L.A.** (1986). Immunogold localization of xyloglucan and rhamnogalacturonan I in the cell walls of suspension-cultured sycamore cells. *Plant Physiol.* **82**: 787–794.
- Moore, P.J., and Staehelin, L.A.** (1988). Immunogold localization of the cell-wall-matrix polysaccharides rhamnogalacturonan I and xyloglucan during cell expansion and cytokinesis in *Trifolium pratense* L.: Implication for secretory pathways. *Planta* **174**: 433–445.
- Moore, P.J., Swords, K.M.M., Lynch, M.A., and Staehelin, L.A.** (1991). Spatial organization of the assembly pathways of glycoproteins and complex polysaccharides in the Golgi apparatus of plants. *J. Cell Biol.* **112**: 589–602.
- Munson, M., and Novick, P.** (2006). The exocyst defrocked, a framework of rods revealed. *Nat. Struct. Mol. Biol.* **13**: 577–581.
- Nebenführ, A., Frohlick, J.A., and Staehelin, L.A.** (2000). Redistribution of Golgi stacks and other organelles during mitosis and cytokinesis in plant cells. *Plant Physiol.* **124**: 135–151.
- Nebenführ, A., Gallagher, L.A., Dunahay, T.G., Frohlick, J.A., Mazurkiewicz, A.M., Meehl, J.B., and Staehelin, L.A.** (1999).

- Stop-and-go movements of plant Golgi stacks are mediated by the acto-myosin system. *Plant Physiol.* **121**: 1127–1142.
- Nebenführ, A., and Staehelin, L.A.** (2001). Mobile factories: Golgi dynamics in plant cells. *Trends Plant Sci.* **6**: 160–167.
- Northcote, D.H., and Pickett-Heaps, J.D.** (1966). A function of the Golgi apparatus in polysaccharide synthesis and transport in the root-cap cells of wheat. *Biochem. J.* **98**: 159–167.
- Odell, J.T., Nagy, F., and Chua, N.H.** (1985). Identification of DNA sequences required for activity of the cauliflower mosaic virus 35S promoter. *Nature* **313**: 810–812.
- Persson, S., Caffall, K.H., Freshour, G., Hille, M.T., Bauer, S., Poindexter, P., Hahn, M.G., Mohnen, D., and Somerville, C.** (2007). The *Arabidopsis* irregular xylem8 mutant is deficient in glucuronoxylan and homogalacturonan, which are essential for secondary cell wall integrity. *Plant Cell* **19**: 237–255.
- Pesacreta, T.C., and Lucas, W.J.** (1985). Presence of a partially-coated reticulum in angiosperms. *Protoplasma* **125**: 173–184.
- Preuss, M.L., Schmitz, A.J., Thole, J.M., Bonner, H.K., Otegui, M.S., and Nielsen, E.** (2006). A role for the RabA4b effector protein PI-4Kbeta1 in polarized expansion of root hair cells in *Arabidopsis thaliana*. *J. Cell Biol.* **172**: 991–998.
- Preuss, M.L., Serna, J., Falbel, T.G., Bednarek, S.Y., and Nielsen, E.** (2004). The *Arabidopsis* Rab GTPase RabA4b localizes to the tips of growing root hair cells. *Plant Cell* **16**: 1589–1603.
- Puhlmann, J., Bucheli, E., Swain, M.J., Dunning, N., Albersheim, P., Darvill, A.G., and Hahn, M.G.** (1994). Generation of monoclonal antibodies against plant cell-wall polysaccharides. *Plant Physiol.* **104**: 699–710.
- Rensing, K.H., Samuels, A.L., and Savidge, R.A.** (2002). Ultrastructure of vascular cambial cell cytokinesis in pine seedlings preserved by cryofixation and substitution. *Protoplasma* **220**: 39–49.
- Roudier, F., Fernandez, A.G., Fujita, M., Himmelspach, R., Borner, G.H.H., Schindelman, G., Song, S., Baskin, T.I., Dupree, P., Wasteneys, G.O., and Benfey, P.N.** (2005). COBRA, an *Arabidopsis* extracellular glycosylphosphatidylinositol-anchored protein, specifically controls highly anisotropic expansion through its involvement in cellulose microfibril orientation. *Plant Cell* **17**: 1749–1763.
- Segui-Simarro, J.M., and Staehelin, L.A.** (2006). Cell cycle-dependent changes in Golgi stacks, vacuoles, clathrin-coated vesicles and multivesicular bodies in meristematic cells of *Arabidopsis thaliana*: A quantitative and spatial analysis. *Planta* **223**: 223–236.
- Sherrier, D.J., and Vandenbosch, K.A.** (1994). Secretion of cell wall polysaccharides in *Vicia* root hairs. *Plant J.* **5**: 185–195.
- Somerville, C., Bauer, S., Brininstool, G., Facette, M., Hamann, T., Milne, J., Osborne, E., Paredes, A., Persson, S., Raab, T., Vorwerk, S., and Youngs, H.** (2004). Toward a systems approach to understanding plant cell walls. *Science* **306**: 2206–2211.
- Spurr, A.R.** (1969). A low-viscosity epoxy resin embedding medium for electron microscopy. *J. Ultrastruct. Res.* **26**: 31–43.
- Staehelin, L.A., Giddings, T.H., Kiss, J.Z., and Sack, F.D.** (1990). Macromolecular differentiation of Golgi stacks in root tips of *Arabidopsis* and *Nicotiana* seedlings as visualized in high pressure frozen and freeze-substituted samples. *Protoplasma* **157**: 75–91.
- Synek, L., Schlager, N., Elias, M., Quentin, M., Hauser, M.T., and Zarsky, V.** (2006). AtEXO70A1, a member of a family of putative exocyst subunits specifically expanded in land plants, is important for polar growth and plant development. *Plant J.* **48**: 54–72.
- Thole, J.M., Vermeer, J.E., Zhang, Y., Gadella, T.W., Jr., and Nielsen, E.** (2008). ROOT HAIR DEFECTIVE4 encodes a phosphatidylinositol-4-phosphate phosphatase required for proper root hair development in *Arabidopsis thaliana*. *Plant Cell* **20**: 381–395.
- Usadel, B., Kuschinsky, A.M., Rosso, M.G., Eckermann, N., and Pauly, M.** (2004). RHM2 is involved in mucilage pectin synthesis and is required for the development of the seed coat in *Arabidopsis*. *Plant Physiol.* **134**: 286–295.
- Wen, T.J., Hochholding, F., Sauer, M., Bruce, W., and Schnable, P.S.** (2005). The roothairless1 gene of maize encodes a homolog of sec3, which is involved in polar exocytosis. *Plant Physiol.* **138**: 1637–1643.
- Wen, T.-J., and Schnable, P.S.** (1994). Analyses of mutants of three genes that influence root hair development in *Zea mays* (Gramineae) suggest that root hairs are dispensable. *Am. J. Bot.* **81**: 833–842.
- Western, T.L., Burn, J., Tan, W.L., Skinner, D.J., Martin-McCaffrey, L., Moffatt, B.A., and Haughn, G.W.** (2001). Isolation and characterization of mutants defective in seed coat mucilage secretory cell development in *Arabidopsis*. *Plant Physiol.* **127**: 998–1011.
- Western, T.L., Skinner, D.J., and Haughn, G.W.** (2000). Differentiation of mucilage secretory cells of the *Arabidopsis* seed coat. *Plant Physiol.* **122**: 345–356.
- Western, T.L., Young, D.S., Dean, G.H., Tan, W.L., Samuels, A.L., and Haughn, G.W.** (2004). MUCILAGE-MODIFIED4 encodes a putative pectin biosynthetic enzyme developmentally regulated by APETALA2, TRANSPARENT TESTA GLABRA1, and GLABRA2 in the *Arabidopsis* seed coat. *Plant Physiol.* **134**: 296–306.
- Willats, W.G., Gilmartin, P.M., Mikkelsen, J.D., and Knox, J.P.** (1999). Cell wall antibodies without immunization: Generation and use of de-esterified homogalacturonan block-specific antibodies from a naive phage display library. *Plant J.* **18**: 57–65.
- Willats, W.G., McCartney, L., and Knox, J.P.** (2001a). In-situ analysis of pectic polysaccharides in seed mucilage and at the root surface of *Arabidopsis thaliana*. *Planta* **213**: 37–44.
- Willats, W.G., Orfila, C., Limberg, G., Buchholt, H.C., van Alebeek, G.J., Voragen, A.G., Marcus, S.E., Christensen, T.M., Mikkelsen, J.D., Murray, B.S., and Knox, J.P.** (2001b). Modulation of the degree and pattern of methyl-esterification of pectic homogalacturonan in plant cell walls. Implications for pectin methyl esterase action, matrix properties, and cell adhesion. *J. Biol. Chem.* **276**: 19404–19413.
- Windsor, J.B., Symonds, V.V., Mendenhall, J., and Lloyd, A.M.** (2000). *Arabidopsis* seed coat development: Morphological differentiation of the outer integument. *Plant J.* **22**: 483–493.
- Zhang, G.F., and Staehelin, L.A.** (1992). Functional compartmentation of the Golgi apparatus of plant cells. *Plant Physiol.* **99**: 1070–1083.

**Analysis of the Golgi Apparatus in Arabidopsis Seed Coat Cells during Polarized Secretion of Pectin-Rich Mucilage**

Robin E. Young, Heather E. McFarlane, Michael G. Hahn, Tamara L. Western, George W. Haughn and A. Lacey Samuels

*PLANT CELL* 2008;20;1623-1638; originally published online Jun 3, 2008;

DOI: 10.1105/tpc.108.058842

This information is current as of October 2, 2008

<b>Supplemental Data</b>	<a href="http://www.plantcell.org/cgi/content/full/tpc.108.058842/DC1">http://www.plantcell.org/cgi/content/full/tpc.108.058842/DC1</a>
<b>References</b>	This article cites 65 articles, 27 of which you can access for free at: <a href="http://www.plantcell.org/cgi/content/full/20/6/1623#BIBL">http://www.plantcell.org/cgi/content/full/20/6/1623#BIBL</a>
<b>Permissions</b>	<a href="https://www.copyright.com/ccc/openurl.do?sid=pd_hw1532298X&amp;iissn=1532298X&amp;WT.mc_id=pd_hw1532298X">https://www.copyright.com/ccc/openurl.do?sid=pd_hw1532298X&amp;iissn=1532298X&amp;WT.mc_id=pd_hw1532298X</a>
<b>eTOCs</b>	Sign up for eTOCs for <i>THE PLANT CELL</i> at: <a href="http://www.plantcell.org/subscriptions/etoc.shtml">http://www.plantcell.org/subscriptions/etoc.shtml</a>
<b>CiteTrack Alerts</b>	Sign up for CiteTrack Alerts for <i>Plant Cell</i> at: <a href="http://www.plantcell.org/cgi/alerts/ctmain">http://www.plantcell.org/cgi/alerts/ctmain</a>
<b>Subscription Information</b>	Subscription information for <i>The Plant Cell</i> and <i>Plant Physiology</i> is available at: <a href="http://www.aspb.org/publications/subscriptions.cfm">http://www.aspb.org/publications/subscriptions.cfm</a>